

Strong double K–K transfer channel in near symmetric collision of Si + Ar at intermediate velocity range

B B Dhal^{†||}, L C Tribedi^{†¶}, U Tiwari[†], P N Tandon[†], T G Lee[‡], C D Lin[‡]
and L Gulyás[§]

[†] Tata Institute of Fundamental Research, Homi Bhabha Road, Colaba, Bombay 400 005, India

[‡] J R Macdonald Laboratory, Department of Physics, Kansas State University, Manhattan,
KS 66506, USA

[§] Nuclear Data Center, Japan Atomic Energy Research Institute, Tokai, Naka, Ibaraki 319-1195,
Japan

E-mail: lokesh@tifr.res.in

Received 11 November 1999, in final form 17 January 2000

Abstract. We present a combined study of single and double K–K electron transfer cross sections along with the single and double K-shell ionization of Ar induced by Si projectiles in the energy range 0.9–4.0 MeV u⁻¹. The charge-state dependence of the normal and hypersatellite x-rays was used to derive the cross sections for the one- and two-electron processes, respectively. The enhancement in the fluorescence yields due to multiple vacancies was measured from the energy shifts and intensity ratios of the characteristic x-ray lines to derive K-shell vacancy production cross sections from x-ray production cross sections. The ratio of double to single K–K transfer cross sections is found to be quite large for this nearly symmetric collision system, whereas the ratio of double to single ionization cross sections is quite small. The measured single K–K transfer cross sections are reproduced very well by the two-centre close-coupling calculations whereas the double K–K transfer data are underestimated by the theory based on the independent-electron approximation (IEA). The K-shell ionization cross sections are found to deviate strongly from the calculations based on the continuum distorted wave eikonal initial state (CDW-EIS) and ECPSSR models. The CDW-EIS calculations along with the IEA model grossly underestimate the double ionization cross sections. It is stressed that in the case of two-electron processes the independent-electron model breaks down and the possible role of correlations between K-electrons is discussed.

1. Introduction

Inner-shell electron transfer in highly charged ions in collision with neutral atoms at intermediate impact velocities is a major vacancy production process in target atoms, and depending on the symmetry of collision systems, in some cases, this channel could be much larger than the direct Coulomb ionization. The initial and final state binding energies of the transferred electron, the symmetry parameter $S_z = Z_1/Z_2$ and the reduced velocity $v_r = v_p/v_e$ of the collision system are the relevant parameters which are generally used to describe the transfer process. Here Z_1 and Z_2 refer to the atomic numbers of the projectile and the target, while v_p and v_e are the velocity of the projectile and the orbital velocity of the active target electron, respectively. The binding energy matching between initial and final states provides a favourable condition for electron transfer as predicted by the first-order calculations. There

^{||} Present address: School of Physics, University of Melbourne, Parkville, Victoria 3052, Australia.

[¶] Author to whom correspondence should be addressed.

exist many measurements on the total electron capture cross sections for initially loosely bound electrons, and several empirical scaling laws (Schlachter *et al* 1983, Knudsen *et al* 1981) have been developed to describe such a process. These cross sections fall rapidly ($\sim v^{-11}$) with the projectile velocity whereas the cross sections for the deeply bound electron transfer (such as σ_{K-K}) process have a maximum at the intermediate velocity range, i.e. for $v_r \approx 1$, as in this study. Moreover, the state-selective electron transfer cross sections involving deeply bound initial and final states cannot be described by such empirical laws. In addition, the mechanism for two-electron processes such as double transfer and double ionization are more involved since these processes may also include a contribution from e-e correlation as well as from the nuclear contribution. Although there have been a lot of experimental and theoretical studies on the ratio of double to single ionization cross sections for heavy ion impact on He to explore the e-e correlation, there are hardly any such studies for the case of double ionization and double transfer of the deeply bound electrons, i.e. with keV binding energies.

To our best knowledge, only a few measurements exist for single and double K-K (Hall *et al* 1983, 1986, Wohrer *et al* 1984, Tribedi *et al* 1993, 1994), L-K electron transfer (i.e. transfer from the L-shell of the target atom to the K-shell of the projectile ion) (Dhal *et al* 1998) and projectile double K-vacancy processes (Tanis *et al* 1980). Most of these experiments have been carried out for asymmetric collision systems by using thin solid targets. As the measured values of the transfer cross sections are quite large, the reported values, even though using thin targets for the measurements, might be dependent on the thickness of the target used due to the initial very steep thickness dependence of the charge state of the ion inside the solid. This is certainly true for incident charge states beyond their equilibrium values in solids (Tribedi *et al* 1993). Therefore, it is desirable to perform measurements on these processes in which the single collision condition is satisfied, i.e. using a low-pressure gas target. The double K-K transfer cross sections generally fall one to two orders of magnitude below those observed for single K-K electron transfer (Hall *et al* 1983). However, in a nearly symmetric collision system the 2K-2K electron transfer channel can be quite a substantial fraction of the single electron transfer process and can therefore provide a critical test to the theoretical models which use the independent-particle approximation (IEA) (see below). However, very limited experimental data are available (Hall *et al* 1986). We have, therefore, carried out single and double electron transfer cross sections for a nearly symmetric collision system Si + Ar ($S_z \sim 0.8$) in the intermediate impact energy range ($0.5 \leq v_r \leq 0.8$) where these cross sections are expected to be near maximum. In addition, we also present the single and double ionization cross sections and K-L transfer cross sections. We compare these data with several theoretical calculations as mentioned below.

It is known that the first-order theory based on the Oppenheimer-Brinkman-Kramer-Nikolaev (OBKN) approximation (Nikolaev 1967) overestimates the electron capture cross sections by a large factor. As an improvement to these calculations, in the perturbed stationary state approach Lapicki and McDaniel (1980) included the second Born term and corrections due to the enhanced binding energy and Coulomb deflection in the OBKN formalism. However, this formalism (perturbed stationary state (PSS)) also overestimates the K-K transfer cross sections for a near-symmetric collision system as considered in this case, and are therefore not discussed. The same calculations are shown for K-L transfer data. *Ab initio* calculations based on the close-coupling method (Kuang and Lin 1996, Fritsch and Lin 1991) with atomic orbitals on the two collision centres (Bates and McCarroll 1958) have been widely used with great success for calculating state-selective electron transfer cross sections involving outer-shell electrons. Within this approach, the motion of the heavy nuclei is approximated by a classical trajectory whereas the target electrons are treated quantum mechanically. For treating electron capture from the inner shells, an independent-electron model is used and the

active electron is described by a model potential fitted so that the binding energy of the active electron is reproduced. In the close-coupling calculation all the atomic states up to $n = 2$ on both centres have been included. Within the independent-electron approximation (IEA), two-electron processes like double K–K transfer cross sections are also calculated. Deviation from the theoretical calculations using this model can provide an important clue to the validity of the IEA model. A near-symmetric collision system in the present velocity range is well suited to probe these aspects owing to its large double K–K transfer probability.

In the case of deeply bound K- and L-shell ionization, it has become conventional to use a calculation such as ECPSSR which is a first-order Born calculation and modified in the PSS approach, i.e. by introducing the corrections due to enhanced binding energy, Coulomb deflection, energy loss and any relativistic effects (Brandt and Lapicki 1981). The attractiveness of this model arises due the use of an analytical expression to calculate the cross section and in the absence of the *ab initio* theoretical calculations. It has also been shown recently that the distorted wave calculations such as continuum distorted wave eikonal initial state (CDW-EIS) calculations developed by Crothers and McCann (1983) and further improved by Fainstein and others (Fainstein *et al* 1991, Gulyás *et al* 1995) have been successful in explaining the double differential ionization cross sections of light atoms in fast ion–atom collisions (Pedersen *et al* 1991, Stolterfoht *et al* 1995, Tribedi *et al* 1998a, b). The CDW-EIS is a first-order distorted wave theory in which the distortion of the projectile in the initial channel is described by an eikonal phase. In the final state the free electron moves in the combined Coulomb field of the projectile and target, giving rise to what is called a two-centre effect. This theory has been demonstrated to be valid far beyond the conventional first Born model for accounting for the differential ionization cross sections of atoms dominated by slightly bound outer-shell electrons by various highly charged projectiles ion impacts (see references above). However, in the present collision system the electrons are much more strongly bound ($v_r \leq 1$) and it is not clear whether the CDW-EIS calculations can explain the ionization data for such a highly non-perturbative collision system. Therefore, we performed the CDW-EIS calculations for K-shell ionization which employ the Hartree–Fock–Slater wavefunctions of the initial and final states of the ionized electron. The double K-ionization cross sections are also calculated using CDW-EIS along with the IEA.

2. Experimental details

An ion beam of ^{28}Si , at energies varying between 27 and 110 MeV, was obtained from the BARC-TIFR Pelletron accelerator at TIFR, Mumbai. The mass and energy analysed beam was passed through a post-acceleration foil stripper to obtain different charge states of the incoming beam at a given energy. The charge-state-selected beam was focused on to a cylindrical gas cell 4 cm long with 2 and 3 mm openings at the entrance and exit of the cell, respectively. The entrance and exit apertures of the gas cell were electrically isolated to facilitate good transmission of the beam focused through it. The emerging beam was collected on a long extended Faraday cup connected to the chamber. The charge collected on the Faraday cup was used for normalization. The cell was differentially pumped and the gas inflow within the cell continuously monitored and controlled at a desired gas pressure with the help of a capacitance manometer and a solenoid valve. The base pressure in the main chamber was maintained at 1×10^{-6} Torr. The emitted x-rays were detected at 90° by two Si(Li) detectors through mylar windows (of thickness $25 \mu\text{m}$) which were fixed on the gas cell and the main chamber. The detector had a resolution of ~ 160 eV at 5.9 keV. A PC-based system along with a CAMAC controller were used for data acquisition. An aperture was placed in front of the detector to accurately define the interaction volume in the gas cell. The thickness of the mylar foil used

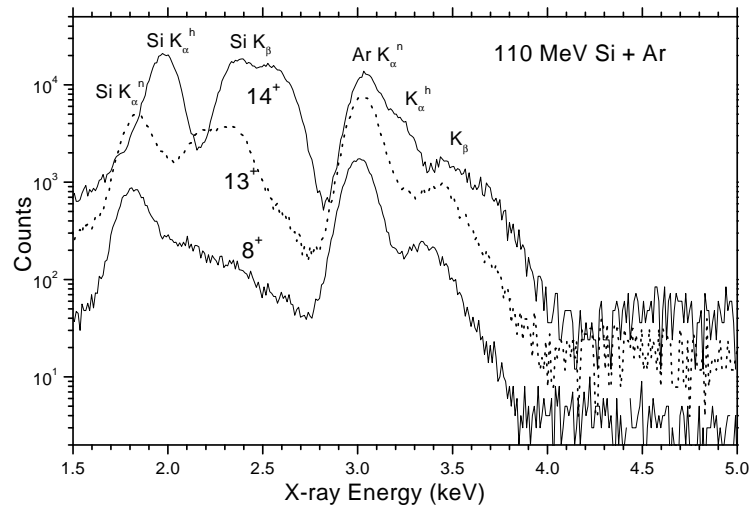


Figure 1. The measured Ar x-ray spectra on bombardment with 110 MeV Si ions with three different charge states of 8^+ , 13^+ (dotted curve) and 14^+ . The normal and hyper components of $K\alpha$ and $K\beta$ in the case of Ar are indicated. The projectile x-rays are also shown.

was determined by measuring the transmission of 3.3 keV x-rays from the ^{241}Am source. The Ar x-ray yield from the interaction volume was measured as a function of the gas cell pressure, and single collision conditions were maintained during the experiment. A typical value of the gas pressure used was about 5 mTorr.

3. Data analysis, results and discussions

Typical x-ray spectra obtained for Ar on impact with Si ions in different charge states are shown in figure 1. The characteristic x-rays arising from Si ions and Ar are widely separated. The x-ray spectra using 8^+ , 13^+ and 14^+ charge states of Si ions, i.e. having zero, one and two vacancies in their K-shell, respectively, are widely different. The dominance of hypersatellite (K^h) components for Si and Ar is very evident when fully stripped Si ions are used as the projectile. The intensity of the K-hypersatellite component is a measure of the double K-vacancy at the time of x-ray emission. The intensities of the $K\alpha^h$ and $K\beta^h$ components for Ar were obtained from a fit to the composite spectrum using a multi-Gaussian peak fitting program. The normalized intensity of the x-ray yield, corrected for the absorption due to the mylar window on the gas cell and the Be window of the detector, was used to obtain the total K x-ray production cross sections. The cross section values measured using the two detectors agreed with one another to within 5–10% at all the measured energies and charge states of the incident projectile. For absolute normalization, the Ar K x-ray yields were measured, in the same geometry, using 56 and 77 MeV F ion beams in different charge states for which the x-ray cross sections are known (Hopkins *et al* 1974). It was found that the cross sections derived from the present measurements were slightly lower (by a factor of 1.3) than those obtained by Hopkins *et al*. However, we have used the existing data of Hopkins *et al* (1974) to normalize our cross section data.

The energies of the $K\alpha$ and $K\beta$ components of Ar x-rays were found to be higher than the line-diagram values (Bearden 1967) due to the presence of multiple vacancies in higher shells. The shifts in the energies of these lines (ΔE_α and ΔE_β), together with their intensity ratios

were used to calculate the number of vacancies (Bhalla 1973) in the L- and M-shells at the time of x-ray emission which was required in order to estimate the fluorescence yield (ω_K). The shift ΔE_α was found to vary between 50–90 eV and ΔE_β between 170–300 eV for different energies and charge states investigated. At a given beam energy the energy shifts were found to increase with the charge states. The details of the energy and charge-state dependence may be found elsewhere. It is worth noting here that in the case of a solid target such a charge-state dependence is not observed since the outer shells of the projectiles reach equilibrium very quickly within a few layers of the solid. The number of vacancies were estimated to vary between 2–5 for the L-shell and upto 5 for the M-shell. The calculated values of the fluorescence yield (Bhalla 1973) were quite insensitive to the number of vacancies and varied between 0.13–0.15, but were still larger than the single-hole value of 0.12. Based on the values of the fluorescence yield ($\omega_K(E, q)$), determined for each vacancy configuration, the total K-shell vacancy production cross sections ($\sigma_{KI}^s = \sigma_{Kx}^s/\omega_K$) were obtained (the superscript ‘s’ stands for the normal or satellite line).

The single and double K–K transfer cross sections were derived from the x-ray production cross sections for different charge states using the procedure described by Hall *et al* (1983, 1986). The total x-ray production cross section can be written in terms of the contributions from the satellite (σ_{Kx}^s) and the hypersatellite (σ_{Kx}^h), i.e. $\sigma_{Kx} = \sigma_{Kx}^s + \sigma_{Kx}^h$. Assuming the fluorescence yields for the single and double K-vacancy states to be the same, the corresponding cross sections for single (denoted by the subscript SKV in what follows) and double K-vacancy (denoted by the subscript DKV in what follows) production cross sections are derived using

$$\sigma_{KI} = \sigma_{KI}^s + \sigma_{KI}^h \quad (1)$$

and

$$\sigma_{DKV} = \sigma_{KI} Y_\alpha^h / Y_\alpha^{\text{tot}} \quad (2)$$

where σ_{KI} is the total K-shell ionization cross section and $Y_\alpha^h/Y_\alpha^{\text{tot}}$ is the ratio of the yields of the hypersatellite component to the total x-ray. The single K-vacancy cross section σ_{SKV} is obtained from the satellite component corrected for the cascade contribution from the double K-vacancy state and is given by

$$\sigma_{SKV}^i = \sigma_{KI}^i - 2\sigma_{DKV}^i. \quad (3)$$

The superscript i ($i = 0, 1$ and 2) refers to the number of K-shell vacancies in the incident ion. The single and double K–K transfer cross sections were then deduced using the relations,

$$\sigma_{K-K} = \sigma_{SKV}^1 - \sigma_{SKV}^0, \quad (4)$$

$$\sigma_{K-K} = \frac{1}{2}(\sigma_{SKV}^2 - \sigma_{SKV}^0), \quad (5)$$

$$\sigma_{2K-2K} = \sigma_{DKV}^2 - 2\sigma_{DKV}^1 + \sigma_{DKV}^0. \quad (6)$$

The charge-state dependence of σ_{KI} , measured at various energies, is shown in figures 2(a) and (b). A small increasing trend in going from low-charge states to high-charge states, is observed and attributed to electron transfer from the K-shell of Ar to higher vacant shells (L) of the projectile. A distinct increase in the x-ray yield for the 12^+ charge state is associated with the metastable state of He-like projectile ions while the sudden rise for 13^+ and 14^+ charge states is linked to the direct K–K electron transfer channel. The dependence of the double K-vacancy cross sections on the initial number of vacancies on the incident ions is shown in figure 3 for two different energies. The hypersatellite yield is quite dominant for bare ions only, and the one or two orders of magnitude enhancement over lower charge states is larger than the corresponding case for the x-ray yields of the satellite line. In the case of filled K-shell projectiles the hypersatellite intensity is quite low and results from the small double ionization

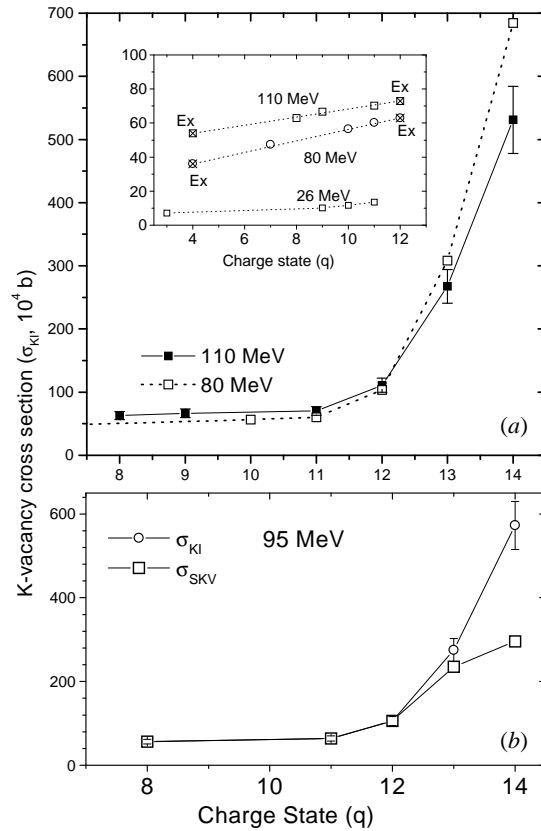


Figure 2. The total K-vacancy production cross section for Ar, σ_{KI} , as a function of the initial charge state of the projectile. The line joining the points is given as a guide to the eye. (a) The data for 110 and 80 MeV. The inset shows the cross sections for zero-K-vacancy ions for 110, 80 and 26 MeV energies along with the extrapolated values at $q = 4^+$ and 12^+ , denoted as 'Ex'. (b) Similar data (circles) for the total K-vacancy cross section for 95 MeV along with the data (squares) for single vacancy cross sections (σ_{SKV}) derived after correcting for the cascade contribution from the double K-vacancy state, i.e. using (3).

probability. In the case of H-like ions, the hypersatellite line arises due to second-order processes such as simultaneous K–K and K–L transfer, simultaneous projectile K-excitation and 2K–2K transfer, as well as double K-ionization. However, the large enhancement in the case of bare ions is mainly due to double K–K transfer.

One should note that the K–K transfer cross section can be derived from either (4) or (5) and the cross sections derived from these two equations are generally the same if the double K–K cross section is quite small compared with the K–K cross section. However, if the double K–K transfer process has an appreciable contribution towards the total K–K transfer, (as in the present case), then the derived value of σ_{K-K} using H-like ions (i.e. (4)) would not be same as that derived using bare ions (i.e. (5)). In the case of bare ions, since the K-vacancy can also be filled via the double transfer process (at the cost of single transfer), the single K–K transfer cross section (per K-vacancy) would be lower than that for H-like ions. This is demonstrated in figure 2(b) in which we have plotted the single vacancy cross sections (squares) which are corrected (σ_{SKV}) for the cascade contribution arising from double K-vacancy states, as given

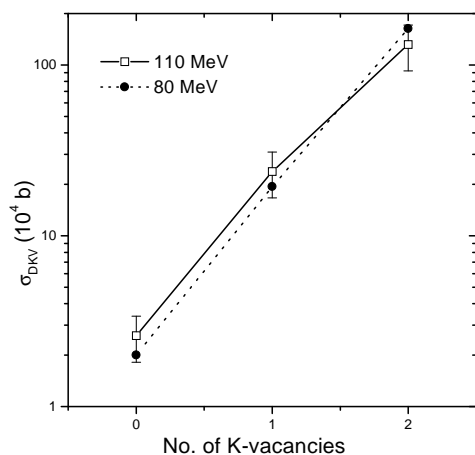


Figure 3. The double K-vacancy cross section (σ_{DKV}) derived as a function of the number of K-shell vacancies on the projectiles for two different energies.

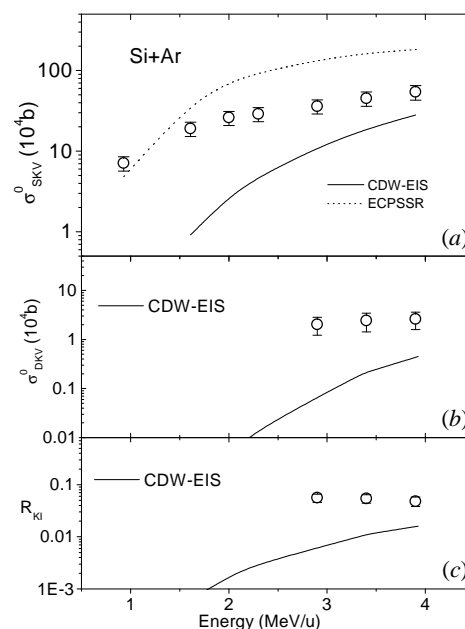


Figure 4. The direct Coulomb ionization cross sections induced by a Si projectile with no initial vacancy in its K-shell (see text) on a Ar target. (a) Single K-vacancy in the Ar K-shell, σ_{SKV}^0 . The dotted curve represents the ECPSSR predictions. (b) Double K-vacancy in the Ar K-shell, σ_{DKV}^0 . (c) The ratio of double to single K-ionization. The solid curves in (b) and (c) show the results of the CDW-EIS calculations.

by (3). The total K-vacancy cross sections (i.e. σ_{KI} in equation (1)) are denoted by circles. One should note that the squares only fall well below the circles for bare ions. It is thus obvious that the single K–K transfer cross sections derived (using (5)) from the cascade corrected data (squares) are lower compared with those derived from the uncorrected ones (circles).

It is apparent from figure 2(a) (and the inset) that for $3 \leq q \leq 12$ there is a steady increase in the cross section as the charge state of the projectile increases. As mentioned earlier, this increase is due to the K–L transfer process, the derived cross sections for which are discussed below. The extrapolated value of the cross sections for $q = 4$ (symbols with crosses), i.e. with no L-shell vacancy, was then used as the K-ionization cross section (plotted as σ_{SKV}^0 in figure 4(a), see below). Similarly, the extrapolated value at $q = 12$ (for correcting the contribution from the metastable state) was used as σ_{SKV}^0 in (4) and (5). The extrapolated points are indicated in the inset of figure 2 and shown as crosses inside the symbols.

The single K-ionization cross sections are compared with ECPSSR calculations in figure 4(a). These calculations overestimate the cross sections throughout the energy range investigated. However, the energy dependence of the cross sections beyond 1.5 MeV u^{-1} agrees well with the calculations. The ECPSSR being a first-order calculation along with the corrective terms fails to explain the data of the present symmetric system. The CDW-EIS calculations underestimate the data at low energies and tend to agree with the measured cross sections at the highest energy investigated. It is worth noting that the CDW-EIS, which takes care of the two-centre effect, explains the double differential and total ionization cross section

data quite well for light targets such as H and He (Tribedi *et al* 1998a, b, Stolterfoht *et al* 1995) in collision with 2–5 MeV u^{-1} bare heavy ions. For these collision systems the perturbation strength parameters ($p = Z_p/v_p$) were small, i.e. in the range 0.4–0.6, and scaled velocity parameters v_r were large, i.e. about 7–10. In contrast, for the present collision, $p = 1.1$ –2, indicating a large perturbation, and v_r falls in the range 0.4–0.7, indicating an adiabatic collision. In this region, the different collision channels such as capture, ionization and excitation become competitive (see the table), and perturbative models become less accurate (Janev *et al* 1985). More elaborate, coupled-channel approaches are necessary which can treat the target and projectile field on an equal footing and account for the strong coupling among the reaction channels. At higher impact energies the perturbative methods become valid and the comparison between the CDW-EIS and data at the highest collision energy indicates that for the present system the theory would explain the data for $v_r \geq 1.0$.

We have also shown in figure 4(b) the derived values for double K-ionization cross sections (σ_{DKV}^0) which increase with the beam energy. One should note that the cross sections for double ionization are only about 5% of those for single ionization and this ratio remains constant with energy. The CDW-EIS calculations fall well below the data and underestimate by a factor of five at the highest energy for which the deviation is minimum. These calculations are carried out using the IEA, i.e. without including the effect of e–e correlation. It remains to be seen whether the inclusion of such a correlation may change the comparison. The difference between the theory and data need not arise entirely from the e–e correlation since the single ionization data themselves are not reproduced by the calculations. However, the ratio of the double to single ionization cross sections ($R_{KI} = \sigma_{DKV}^0/\sigma_{SKV}^0$) should reflect the possible role of e–e correlation and is shown in figure 4(c). The CDW-EIS underestimates the data by at least a factor of three at the highest energy, again indicating the deviation from the IEA model and the limitation of the perturbation approach.

The measured K–K transfer cross sections (per K-vacancy) (figure 5(a)) show a broad maximum at about 60 MeV and then decrease with energy. The open and filled squares represent the cross sections derived using H-like (4) and bare ions (5). The two-centre close-coupling calculations are presented for comparison with the experimental data. Theory and experiment are in good agreement in the sense that the theoretical cross sections pass through the experimental values derived from H-like ions within the error bars for all the energies. A small deviation (about 25%) can be seen at lower energies and agreement is perfect at higher energies. However, the theory overestimates the single transfer cross sections derived from fully stripped ions. It can be seen that data for bare ions fall below those for H-like ions. This is reasonable because for bare ions the K-vacancies can be filled by either double or single K–K transfer channels, whereas in the case of H-like ions the K-vacancies can only be filled by single K–K transfer processes. The theory calculates the single transfer process in an IEA which provides good agreement with H-like data.

In the case of bare ions, the theory overestimates the single transfer data and underestimates the double K–K transfer cross sections (figure 5(b)). In the energy region investigated, the 2K–2K transfer cross sections decrease with increasing projectile energy (figure 5(b)). The theory provides a good qualitative agreement although it underestimates experimental values at lower energies. The good agreement in the case of single K–K transfer cross sections (for H-like ions), the overestimation of single transfer data for bare ions and underestimation of the double transfer data by about 30–40% are indicative of the limitation of using the IEA model in describing these processes (Shingal and Lin 1991). Since the K–K transfer cross sections are defined as per K-vacancy (see (5)) they have to be multiplied by a factor of two before one can take the ratio with the double K–K transfer cross section which can only be achieved for bare ions. In figure 5(c), we show a plot of the ratio $R = \frac{\sigma_{2K-2K}}{2\sigma_{K-K}}$ along with the close-

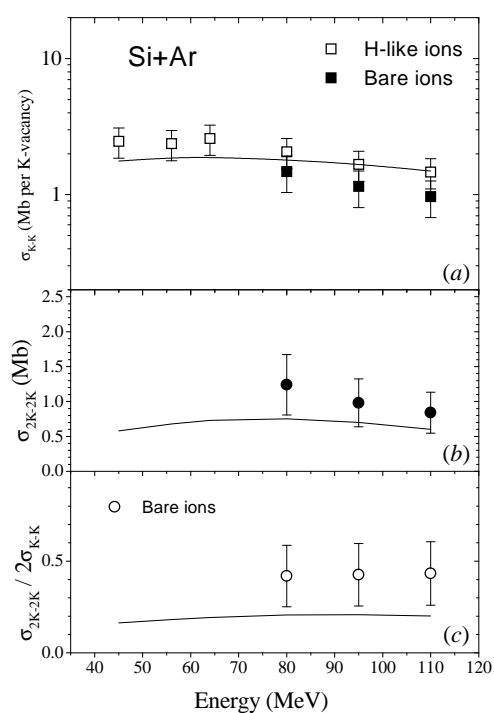


Figure 5. (a) The derived values of the single K–K electron transfer cross sections for H-like (open squares) and bare (filled squares) Si ions on Ar (derived using (4) and (5), respectively). The curve represents the predictions of close-coupling calculations. (b) The derived values of double K–K electron transfer cross sections. The solid curve represents the prediction of CC calculations. (c) The measured ratio of double to single electron transfer cross sections along with the predictions of close-coupling calculations (solid curve).

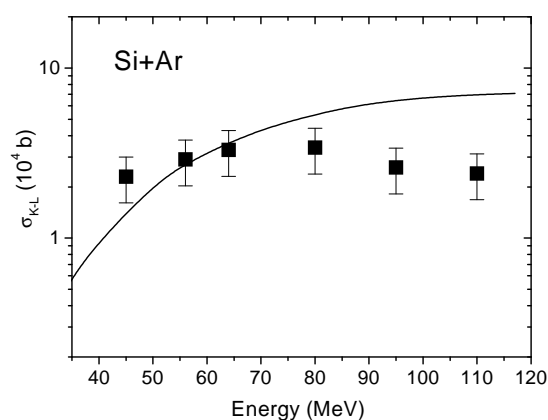


Figure 6. (a) The derived values of the K–L electron transfer cross sections per vacancy (symbols) and the calculations (curve) by Lapicki and McDaniel (1980).

coupling calculation. The observed ratio is shown to be almost independent of energy and is substantially large, i.e. about 42%. This may indicate that for symmetric collisions with bare ions the double K–K transfer channel may be nearly as strong as single K–K transfer (i.e. R approaches 0.5). The theory also shows a nearly energy-independent ratio but underestimates the observed ratio by nearly 50%.

One should note that the calculations used for double ionization or double K–K transfer processes do not include e–e correlation effects and one therefore requires an *ab initio* many-electron theory to understand such inner-shell processes.

The derived values of K–L transfer cross sections (per L-vacancy) are plotted in figure 6 along with the perturbed stationary state calculations of Lapicki and McDaniel (1980). The experimental cross sections increase slowly until 60–70 MeV, above which they start to fall

Table 1. Derived values of single K-ionization (σ_{SKV}^0), double K-ionization (σ_{DKV}^0), double K–K transfer (σ_{2K-2K}) and K–L transfer (σ_{K-L}) cross sections for Si + Ar at various energies. The σ_{K-K}^1 and σ_{K-K}^2 are the K–K transfer cross sections per vacancy derived from H-like (i.e. (4)) and bare ions (i.e. (5)), respectively. The errors in the single and double ionization cross sections are about 20 and 30%; in the K–K and K–L transfer cross sections the errors are about 25 and 30%, and are in the region of 30–35% for the double K–K transfer data.

Energy (MeV)	σ_{K-K}^1 (Mb)	σ_{K-K}^2 (Mb)	σ_{2K-2K} (Mb)	σ_{SKV} (10^4 b)	σ_{DKV}	σ_{K-L} (10^4 b)
26	—	—	—	7.1	—	0.8
45	2.47	—	—	19.0	—	2.3
56	2.37	—	—	26.0	—	2.9
64	2.59	—	—	29	—	3.3
80	2.09	1.48	1.24	36	2.0	3.4
95	1.81	1.15	0.98	45	2.4	2.6
110	1.59	0.97	0.84	54	2.6	2.4

and the theoretical calculations tend to increase with energy in the given range causing a large deviation (about a factor of two) at higher energies. However, at lower energies the calculations agree with the data. It may be mentioned here that the same calculations overestimate the K–K transfer data grossly throughout the energy range, and are not shown here. In order to check the present calculations we have also reproduced the sample calculations provided by Lapicki and McDaniel (1980). The measured ionization cross sections and the transfer cross sections are tabulated in table 1.

4. Conclusions

We have presented a combined study of single and double K-ionization and single and double K–K electron transfer cross sections for Ar induced by ^{28}Si projectiles in the energy range 0.9–4.0 MeV u^{-1} . We have observed the ratio of double to single electron transfer cross sections to be as large as 42% as compared with the single transfer channel, whereas the ratio of double to single K-ionization is only about 5%. The ECPSSR calculations show large deviations from the measured single vacancy production cross sections, overestimating the data. A comparison with the CDW-EIS calculation has also been performed and it is concluded that the theory largely underestimates the data for the presently considered nearly symmetric collision system with a reduced velocity of less than 1.0. The observed double ionization cross section is quite large compared with the CDW-EIS calculations based on the IEA model. The single electron transfer cross sections are reasonably well explained by the semiclassical close-coupling calculations though some deviations are observed for the double transfer process. The disagreement between the double transfer data and the calculation based on the IEA indicates the breakdown of the independent-electron model. We need to formulate an *ab initio* many-electron theory for Coulomb ionization for such deeply bound shells and strongly perturbative collision systems. In addition, the K–L electron transfer cross sections have been derived and compared with theoretical models based on the perturbed stationary state approach.

Acknowledgments

The authors thank A K Saha for his help in the initial stages of this work, K V Thulasiram and S D Narvekar for the technical help and the accelerator staff for smooth operation of the Pelletron accelerator.

References

- Bates D R and McCarroll 1958 *Proc. R. Soc. A* **245** 175
Bearden J A 1967 *Rev. Mod. Phys.* **39** 78
Bhalla C P 1973 *Phys. Rev. A* **8** 2877
Brandt W and Lapicki G 1981 *Phys. Rev. A* **23** 171 and references therein
Crothers D S F and McCann J F 1983 *J. Phys. B: At. Mol. Phys.* **16** 3229
Dhal B B, Saha A K, Tribedi L C, Prasad K G and Tandon P N 1998 *J. Phys. B: At. Mol. Opt. Phys.* **31** L807
Fainstein P D, Ponce V H and Rivarola R D 1991 *J. Phys. B: At. Mol. Opt. Phys.* **24** 3091
Fritsch W and Lin C D 1991 *Phys. Rep.* **202** 1
Gulyás L, Fainstein P D and Salin A 1995 *J. Phys. B: At. Mol. Opt. Phys.* **28** 245
Hall J, Richard P, Gray T J, Newcomb J, Pepmiller P, Lin C D, Jones K, Johnson B and Gregory D 1983 *Phys. Rev. A* **28** 99
Hall J, Richard P, Pepmiller P L, Gregory D C, Miller P D, Moak C D, Jones C M, Alton G D, Bridwell L B and Sofield C J 1986 *Phys. Rev. A* **33** 914
Hopkins F, Brenn R, Whittemore R, Cue N, Dutkiewicz V and Chaturvedi 1974 *Phys. Rev. A* **13** 74
Janev R K, Presnyakov L P and Shevelko V P 1985 *Physics of Highly Charged Ions (Springer Series on Electrophysics vol 13)* (Berlin: Springer)
Knudsen H, Haugen H K and Hvelplund P 1981 *Phys. Rev. A* **23** 597
Kuang J and Lin C D 1996 *J. Phys. B: At. Mol. Opt. Phys.* **29** 1207
Lapicki G and McDaniel F D 1980 *Phys. Rev. A* **22** 1896
Nikolaev V S 1967 *Sov. Phys.–JETP* **24** 847
Pedersen J O P, Hvelplund P, Petersen A and Fainstein P 1991 *J. Phys. B: At. Mol. Opt. Phys.* **24** 4001
Schlachter A S, Stearns J W, Graham W G, Berkner K H, Pyle R V and Tanis J A 1983 *Phys. Rev. A* **27** 3372
Stolterfoht N, Platten H, Schiwietz G, Schneider D, Gulyás L, Fainstein P D and Salin A 1995 *Phys. Rev. A* **52** 3796
Shingal R and Lin C D 1991 *J. Phys. B: At. Mol. Opt. Phys.* **24** 251
Tanis J A, Shafroth S M, Willis J E and Morwat 1980 *Phys. Rev. Lett.* **45** 1547
Tribedi L C, Prasad K G and Tandon P N 1993 *Phys. Rev. A* **47** 3739
Tribedi L C, Prasad K G, Tandon P N, Chen Z and Lin C D 1994 *Phys. Rev. A* **49** 1015
Tribedi L C, Richard P, DeHaven W, Gulyás L, Gealy M W and Rudd M E 1998a *J. Phys. B: At. Mol. Opt. Phys.* **31** L369
Tribedi L C, Richard P, Wang Y D, Lin C D, Gulyás L and Rudd M E 1998b *Phys. Rev. A* **31** 3619
Wohrer K, Chetoui A, Rozet J P, Jolly A and Stephan C 1984 *J. Phys. B: At. Mol. Opt. Phys.* **17** 1575